International Journal of Automotive Technology, Vol. 24, No. 6, pp. 1627−1641 (2023)
DOI 10.1007/s12239−023−0131−5

pISSN 1229−9138/ eISSN 1976−3832

MULTI-OBJECTIVE VELOCITY TRAJECTORY OPTIMIZATION METHOD FOR AUTONOMOUS MINING VEHICLES

Shuwei Pei and Jue Yang*

School of Mechanical Engineering, University of Science and Technology Beijing, Beijing 100083, China

(Received 7 March 2023; Revised 5 August 2023; Accepted 6 September 2023)

ABSTRACT−Autonomous mining transportation is an intelligent traffic control system that can provide better economics than traditional transportation systems. The velocity trajectory of a manned vehicle depends on the driver's driving style. Still, it can be optimized utilizing mathematical methods under autonomous driving conditions. This paper takes fuel and electric mining vehicles with a load capacity of 50 tons as the subject. It contributes a multi-objective optimization approach considering time, energy consumption, and battery lifetime. The dynamic programming (DP) algorithm is used to solve the optimal velocity trajectory with different optimization objectives under two types of mining condition simulation. The trajectories optimized by the single objective, energy consumption, usually adopt the pulse-and-gliding (PnG) approach frequently, which causes the battery capacity loss and increases the travel time. Hence, a multi-objective optimization approach is proposed. For electric vehicles, trajectories optimized by the multi-objective approach can decrease the battery capacity loss by 22.01 % and the time consumption by 41.28 %, leading to a 42.12 % increment in energy consumption. For fuel vehicles, it can decrease the time consumption by 32.54 %, leading to a 7.68 % increment in energy consumption. This velocity trajectory is smoother with less fluctuation. It can better meet the requirements of mining transportation and has a particular reference value for optimizing autonomous transportation costs in closed areas.

KEY WORDS : Velocity trajectory, Energy consumption, Transportation efficiency, Multi-objective optimization

1. INTRODUCTION

To maximize the economy and total transportation volume under limited resources such as the number of vehicles and time consumption. In conventional manned vehicles, the overall transport cost is mainly related to the driver's driving habits and experience. Velocity optimization of vehicles is one of the main eco-driving techniques, which has excellent potential to extend the powertrain capability and automatic longitudinal control by minimizing energy consumption. Figure 1 illustrates the graph showing a real-life human-driven velocity profile under certain road conditions. A clear linear relationship exists between time consumption and distance, and plenty of space for cost optimization throughout the traveling. An essential difference between the autonomous mining transportation system and the traditional transportation system is that the velocity trajectory of autonomous vehicles can be optimized by detailed route information and vehicle characteristic. Therefore, in autonomous mining transportation system, some researchers have demonstrated that energy consumption, emissions, transportation efficiency and other performances have much room for improvement on the basis of different optimization methods.

In recent years, eco-driving has drawn increasing attention from researchers on both urban roads and haulage activities. Velocity optimization gradually becomes a hot research topic with great potential to improve transportation efficiency and energy consumption. Gilbert (1976) initially demonstrated mathematically that Periodic Control outperformed the quasi-relaxed steady state (QRSS) method for cruising conditions. This conclusion overturned the principle that a constant speed (CS) driving trajectory had the best fuel consumption. Xu *et al*. (2015) used the

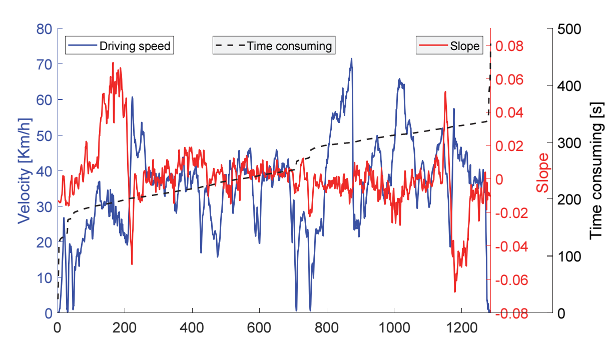

Figure 1. Driver's real driving velocity profile.

*Corresponding author. e-mail: yangjue@ustb.edu.cn

Legendre pseudo-spectral method to quantify the economical cruising trajectories for vehicles equipped with a step-gear transmission and a gasoline engine. It is proved that pulse-and-gliding (PnG) operation had significant fuel saving compared with the constant-speed cruising trajectory. Guo *et al*. (2019) proposed a hierarchical control strategy of velocity optimization to reduce computation time and energy consumption. It is also shown that an improvement of 30 % in fuel economy is achieved compared with the real-life human-driven velocity profiles.

Many different approaches are used to optimize energy consumption. An equivalent consumption minimization strategy is provided to optimize energy management for series-parallel PHEV city buses. It showed a fuel economy improvement of 8.2 % in the Chinese Bus Driving Cycle compared with the validated rule-based energy control strategy (Cai *et al*., 2017). Kusuma *et al*. (2021) found that the minimum energy consumption can be achieved by adopting a serial regenerative braking strategy to save up to 15 % of energy. An adaptive energy management strategy was proposed for multiple energy sources. Dynamic programming (DP) was employed to develop optimal control strategies, which had better efficiency than conventional DP-based strategies (Zhang and Xiong, 2015). Deep Q learning was adopted and verified for energy management issues (Wu *et al*., 2018). It performed better in training time consumption and convergence rate and demonstrated the fuel economy achieved 89 % of DP-based method. (De Cauwer *et al*., 2019) also presented an integrated model for energy consumption and range estimation capable of energy-efficient routing. It showed that energy-efficiency gains up to 37 %. Ma *et al*. (2019) tested and verified the newly developed algorithms using Relaxed Pontryagin's Minimum Principle (RPMP) on an innovative, connected, and automated vehicle platform. Experimental data showed that more than 20 % of fuel consumption could be saved. In addition, the driving style is considered to improve energy consumption, travel time, and comfortable. Hu *et al*. (2022) obtained trajectory clusters reflecting the driver's driving style by trajectory data mining and proposed a speed trajectory optimization method based on driving style finally, which reduced energy consumption significantly.

To sum up the mentioned works of literature, no matter which factor these researchers focus on, the core problem is to solve the velocity profile optimization and energy allocation problem from the origin to the destination. However, it is difficult to optimize the whole velocity trajectory in real-world driving scenarios because it is a very complex problem with multi factors. Previous research on velocity and energy optimization seldom conduct different cost components. In addition, time consumption for the whole mining shift is an essential factor that can improve efficiency and economy, and battery health is also considered as an optimization objective to maintain a long lifetime for electric vehicles. Many factors are conflicting. Reduction in energy consumption leads to an increase in travel time, and the braking recovery system also causes more damage to battery health. Thus, velocity optimization is a multi-objective and nonlinear optimal control problem due to the complex factors and cost functions.

The multi-objective optimization strategy is proposed in this paper. The main contributions of this paper are from three perspectives:

(1) Considering energy, efficiency, and battery health, a multi-objective velocity trajectory optimization method for fuel and electric vehicles is built based on physical constraints.
(2) DP is employed to handle multi-objective velocity trajectory optimization problems because of guaranteed global optimality.
(3) Velocity trajectories optimized by single energy objective and multi-objective are analyzed to reveal the trade-off between energy, time, and battery loss, contributing to achieving a desired mining transportation cost requirement.

The remainder of this paper is organized as follows. Section 2 formulates the open-pit velocity trajectory optimization problem and introduces the DP method. In Section 3, electric and fuel vehicle modelings are given, which are then used to solve the optimization problem. Section 4 applies these models and approaches to identify the optimization velocity trajectory. Section 5 analyses the results, and Section 6 concludes the paper.

2. VELOCITY TRAJECTORY OPTIMIZATION PROBLEM STATEMENT

Since the mine's condition of vehicles is cautious due to the limitation of resources such as the number of vehicles and working hours, vehicles should be efficiently operated under available and feasible operation conditions. The shorter the operation time requires, the higher the energy consumption is. Furthermore it also causes some damage to the powertrain for both fuel and electric vehicles, in general. Therefore, the traveling time and energy consumption must be optimized to achieve an economical and reasonable state.

2.1. Introduction of Mining Operating Condition

Open-pit mine transportation is a cyclic operation, including uploading, full-load transportation, unloading, and empty-load transportation, which can be divided into two types: full-load uphill and full-load downhill. The open-pit mine area has a real condition, as shown in Figure 2. Road gradient generally does not exceed 12 %. Because of the unique working environment, this research established two types of fixed driving routes for long-time uphill and downhill working conditions, as shown in Figure 3.

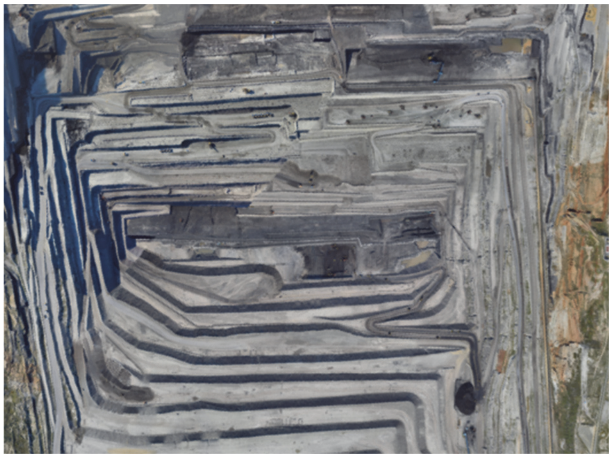

Figure 2. Real condition of the open-pit mine area.

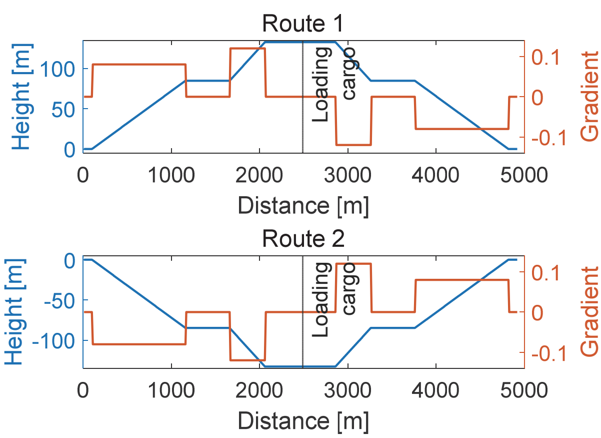

Figure 3. Two types of mining routes.

Table 1. Details of two types of routes.

Distance [m]	Route 1: Gradient	Route 2: Gradient	Load
0 ~ 100	0	0	Empty
100 ~ 1160	0.08	-0.08	Empty
1160 ~ 1660	0	0	Empty
1660 ~ 2060	0.12	-0.12	Empty
2060 ~ 2460	0	0	Empty
2460 ~ 2860	0	0	Full
2860 ~ 3260	-0.12	0.12	Full
3260 ~ 3760	0	0	Full
3760 ~ 4820	-0.08	0.08	Full
4820 ~ 4920	0	0	Full

The total mileage of the two paths is about 4900 meters with a maximum slope of 12 %, and the operation is round-trip. In the first road condition, the vehicle climbs to the top of the hill with an empty load, stops to load, and then returns downhill to the starting point with a full load. Another is where the vehicle rises to the top with an empty load, stops to dump, and then returns downhill to the starting point with a full load. The maximum velocity of vehicles in the mine area is 30 km/h. Detailed Road data are shown in Table 1. The goal is to find a desired solution to make vehicles operate in a proper and economic state.

2.2. Solution Algorithm: Dynamic Programming (DP)

DP is a numerical method for solving optimization problems over plain recursion, which was proposed by the American mathematician Bellman in 1951. As in Figure 4, The idea of DP is to store the results of subproblems so that we do not have to re-compute them when needed later. It refers to simplifying a complicated problem by breaking it down into simpler sub-problems in a recursive manner.

First, the velocity optimization problem is divided into sub-problems according to the distance. If the segmentation distance is too small, it will bring more sub-problems and cause too much computation. The path is divided into sections by the minimum velocity change, considering the relationship between computation time and accuracy. Next,

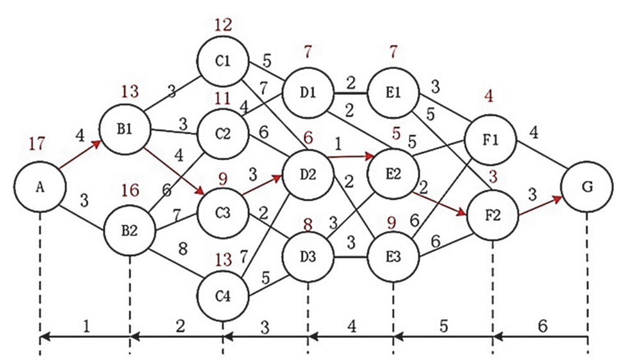

Figure 4. Idea of the DP algorithm.

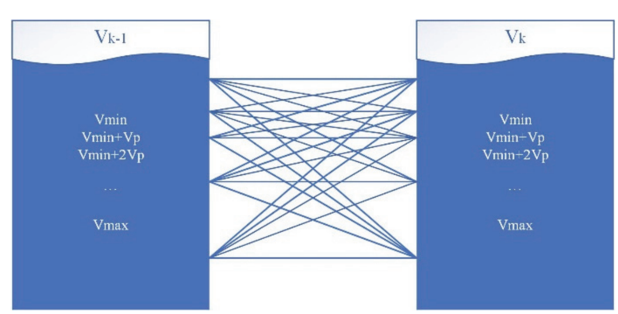

Figure 5. Discretization of velocity in one section.

the velocity is discretized, as shown in Figure 5. Each initial and final velocity of the road section can be freely combined. Finally, this section's acceleration, time, and energy consumption for all possible conditions can be calculated. The value of objective functions can be obtained meanwhile. The best result of each section will be stored and added to the next section as the initial state. After all the sections have been calculated, the minimum value of the last section's results is chosen as the clue to find out the values of previous sections in reverse.

3. VEHICLE CONFIGURATION AND MODELS

In this section, dynamic models for fuel and electric vehicles are formulated. Both vehicle models are established and simulated in MATLAB. The critical parameters of components in vehicles are discussed in the following.

3.1. Powertrain Configuration

Two kinds of vehicles are adopted as the research platform. Both payloads are 45 tons. One is the fuel vehicle with an engine, transmission, and hydraulic braking system. The transmission is AMT with six gears. The critical parameters of the fuel vehicle are shown in Table 2. Another one is the electric vehicle, whose powertrain consists of a battery, motor, transmission, and braking system. Its transmission only has four gears to meet the demand of the driving force. The motor also can be worked as a generator when recovering braking energy. The details of the electric vehicle are shown in Table 3.

Nevertheless, there is a difference between fuel and electric vehicles when braking. For fuel vehicles, it brakes by hydraulic braking system mechanically. While in terms of the electric vehicle, there are two braking conditions. When the braking severity is slight or medium, the vehicle is in regenerative braking condition, where the energy is recovered by the motor and stored in the battery. Otherwise, when the braking severity is high and exceeds the energy recovery ability, the mechanical braking system is activated, working together with the generator to ensure vehicle security.

3.2. Longitudinal Dynamic Model of Vehicle

The mining vehicle studied in this paper has a heavy load capacity, low speed, and simple working conditions. Driving stability and comfort of the vehicle are ignored. Therefore, the longitudinal dynamics model of vehicles is shown in Figure 6. F_i is gradient resistance, F_j represents accelerating resistance, and F_{aero} is air drag, F_{roll} and F_{trac} denote rolling resistance and driving force.

$$F_i = mg\sin\theta$$
$$F_{roll} = fmg\cos\theta \tag{1}$$
$$F_{aero} = \frac{1}{2}C_D A\rho u^2$$

where g is the gravity, θ is the road grade, f represents the coefficient of rolling resistance, C_D is the aerodynamic drag coefficient, A is the vehicle's frontal area, and ρ is the air density.

Those forces whose directions are consistent with the vehicle's speed are taken as positive values. The final equation of the driving force F_{trac} is as follows:

$$F_{trac} \geq F_i + F_j + F_{aero} + F_{roll} \tag{2}$$

Table 2. Details of the fuel vehicle.

Category	Value	Note
Curb weight	34000 kg	-
Payload	45000 kg	-
Engine	389 kW	Maximum
Rolling resistance coefficient	0.02	
Aerodynamic drag coefficient	0.6	
Frontal area	14.84 m^2	
Transmission	Six gears	4 2 2.68 2.01 1.35 1 0.67
Final drive gear ratio	17.83	-
Radius of the tire	0.873 m	Type: 21.00 ~ 35

Table 3. Details of the electric vehicle.

Category	Value	Note
Curb weight	37000 kg	-
Payload	45000 kg	-
Motor	450 kW	Maximum
Rolling resistance coefficient	0.02	
Aerodynamic drag coefficient	0.6	
Frontal area	14.84 m^2	
Transmission	Four gears	8.39 4.34 2.27 1
Final drive gear ratio	17.83	-
Radius of the tire	0.873 m	Type: 21.00 ~ 35
Battery capacity	228 Ah	192s3p

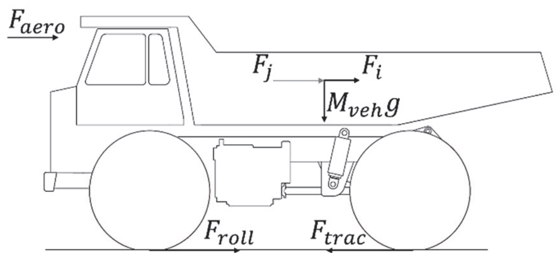

Figure 6. Vehicle longitudinal dynamics model.

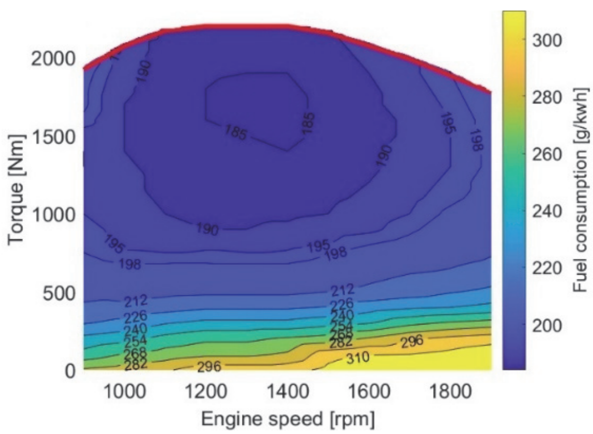

Figure 7. Engine external characteristic curve and brake-specific fuel consumption map.

The vehicle can run properly only if it satisfies this Equation (2).

If $F_{trac} > 0$, the vehicle is in acceleration mode. With the velocity increasing, the sum of each vehicle resistance gradually becomes more considerable. The vehicle velocity will achieve a peak progressively when the sum of resistance exceeds the driving force. If $F_{trac} = 0$ or $F_{trac} < 0$, the vehicle is in gliding or slowing down mode. The vehicle will decelerate, and demand power is negative at this time. Especially for the electric vehicle, the motor starts working as a generator, converting kinetic energy into electricity to charge the battery.

3.3. Engine Model

Engine mechanical constraints include engine output torque and speed limits. Engine fuel consumption can be expressed as a function of the engine torque and speed, as shown in Equation (3). The engine external characteristic curve and brake-specific fuel consumption map are shown in Figure 7.

$$Fuel = f(T_{ICE}, n_{ICE}) \tag{3}$$

where T_{ICE} and n_{ICE} are the torque and rotation speed of the engine.

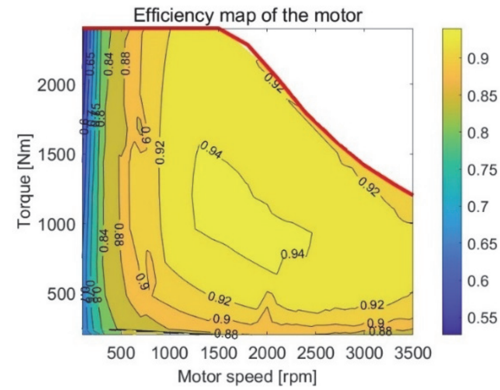

Figure 8. External characteristic curve and efficiency map of the motor.

3.4. Electric Motor Model

The electric motor can be used as the generator to recover energy during vehicle braking. The electrical power drawn from the battery by the electrical machine can be modeled as

$$P_{Gen/Tra} = \eta_{Mot} T_{Gen/Tra} n_{Gen/Tra} \tag{4}$$

where P_{Tra} is the traction motor power, and P_{Gen} is the generator power when it works as the generator. η_{Mot} is the efficiency of the electric motor. $T_{Gen/Tra}$ and $n_{Gen/Tra}$ are the torque and the rotation speed of the motor. The efficiency of the motor of the electrical machine is dynamically adjusted concerning its speed and torque, as shown in Equation (5). The motor's external characteristic curve and efficiency map is shown in Figure 8.

$$\eta_{Mot} = f(T_{Gen/Tra}, n_{Gen/Tra}) \tag{5}$$

3.5. Battery Model

The power flow from and to the battery can be modeled as

$$P_{bat} = \begin{cases} \eta_{dis} P_{ele}, P_{ele} > 0 \\ \eta_{cha} P_{ele}, P_{ele} \le 0 \end{cases} \tag{6}$$

where P_{bat} is the battery power, η_{dis} is the efficiency of the discharge, and η_{cha} is the efficiency of the charge.

Figure 9 shows the simple battery model. Equations (7) and (8) can calculate the battery SOC and power demand.

$$SOC = SOC_O + \frac{\int_{t_o}^{t} I(t)dt}{3600 Q_{max}} \tag{7}$$

$$P_{bat} = V_L I = V_{OC} I + R_{eq} I^2 \tag{8}$$

where SOC_O is the initial SOC, Q_{max} is the battery capacity, I is the current flow, V_L is the output voltage of the battery, V_{OC} is the battery's open-circuit voltage, and R_{eq} is the equivalent internal resistance of the battery.

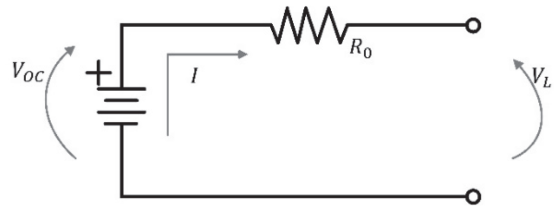

Figure 9. Equivalent circuit of battery.

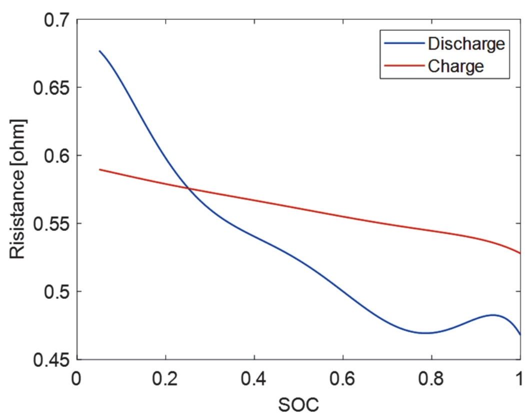

Figure 10. Battery resistance.

The resistance can be described by Equation (9), and the data for the resistance are shown in Figure 10.

$$R_{eq} = \begin{cases} R_{cha}(SOC,T), I < 0 \\ R_{dis}(SOC,T), I > 0 \end{cases} \tag{9}$$

4. OPTIMIZATION

Moreover, velocity trajectory optimization includes many aspects, such as travel time, energy consumption, and battery loss. They are interconnected with each other, especially in the transportation system. Xu *et al*. (2019) proposed a double-layer speed optimization method with the Dijkstra algorithm and real-time computation that considered traffic signal information to decrease fuel consumption and trip time. Zhu *et al*. (2019) proposed an energy-saving path-planning method for EVs considering traffic information. The experimental results showed that it uses lower energy consumption and shorter travel time than the distance-based path and lower energy consumption and longer travel time than the time-based path. Patterson *et al*. (2017) demonstrated that the interconnected relationship between waiting time and truck selection could minimize energy consumption in the mine and contributed an original mixed integer linear programming formulation that scheduled haulage activity to reduce truck and shovel energy consumption. Dehkordi *et al*. (2022) developed a multi-objective optimization methodology to concurrently minimize fuel consumption, travel time, and safety risk based on network-level safety measures, which improved fuel efficiency while simultaneously reducing safety risks. Then, Liu *et al*. (2023) proposed a multi-objective regenerative braking control strategy based on the pseudospectra method with terminal constraints. The control strategy optimized both the velocity and braking torque allocation to reduce the energy dissipation and battery capacity loss simultaneously, which assisted in finding a desired balanced solution.

In this section, single-objective simulations considering energy consumption are first carried out under the mining scenario. The multi-objective optimal mathematical model is constructed with "time consumption," "energy consumption," and "battery lifetime" as the optimization objectives. Thus, the velocity is optimized by a multi-objective approach.

4.1. Single-objective Optimization

The composition of haulage system costs is highly complex. It mainly includes transportation time, energy consumption, wear, and equipment depreciation. The single-objective function considering energy consumption is shown as follows:

$$J = J_{en} = \int_{s_0}^{s_f} P_{out} \frac{ds}{u} \tag{10}$$

where P_{out} is the output power of the vehicle, s_f is the total traveling distance, and u represents the vehicle velocity. Besides, the powertrain components of fuel and electric vehicles are different. T_{ICE} and T_{Mot} are the output torque of the engine and motor. n_{ICE} and n_{Mot} represent the rotational speed of the engine and motor. i_g is the gear ratio of the transmission. The physical constraints of fuel and electric vehicles are shown in Equations (11) and (12), respectively.

$$\begin{aligned} &T_{ICE\_min} < T_{ICE} < T_{ICE\_max} \\ &n_{ICE\_min} < n_{ICE} < n_{ICE\_max} \\ &i_g \in \{i_{g1}, i_{g2}, i_{g3}, i_{g4}, i_{g5}, i_{g6}\} \end{aligned} \tag{11}$$

$$\begin{aligned} &T_{Mot\_min} < T_{Mot} < T_{Mot\_max} \\ &n_{Mot\_min} < n_{Mot} < n_{Mot\_max} \\ &SOC_{min} < SOC < SOC_{max} \\ &i_g \in \{i_{g1}, i_{g2}, i_{g3}, i_{g4}\} \end{aligned} \tag{12}$$

The fuel consumption and SOC change are vital factors of the transportation cost, which can be calculated through the power output according to the engine, motor, and battery characteristics. Thus, the single-objective optimal control problems of fuel and electric vehicles are formulated as Equations (13) and (14).

$$
\begin{aligned}
&J = J_{Fuel} = \int_{s_0}^{s_f} Fuel \cdot P_{out} \frac{ds}{u} \\
&s.t. \\
&\frac{du}{ds} = \frac{F_{trac} - F_i - F_j - F_{aero} - F_{roll}}{mu} \\
&a = \frac{udu}{ds} \\
&T_{ICE} = \frac{F_{trac}R_{tire}}{i_g i_f} \\
&T_{ICE\_min} < T_{ICE} < T_{ICE\_max} \\
&n_{ICE} = \frac{u i_g i_f}{2\pi R_{tire}} \\
&n_{ICE\_min} < n_{ICE} < n_{ICE\_max} \\
&i_g \in \{i_{g1}, i_{g2}, i_{g3}, i_{g4}, i_{g5}, i_{g6}\} \\
&a_{min} < a < a_{max} \\
&0 < u < u_{max}
\end{aligned} \tag{13}
$$

$$
\begin{aligned}
&J = J_{Elec} = \int_{s_0}^{s_f} \frac{U_{OC} - \sqrt{U_{OC}^2 - 4P_{bat}R_{eq}}}{2R_{eq}Q_{max}} \frac{ds}{u} \\
&s.t. \\
&\frac{du}{ds} = \frac{F_{trac} - F_i - F_j - F_{aero} - F_{roll}}{mu} \\
&a = \frac{udu}{ds} \\
&T_{Mot} = \frac{F_{trac}R_{tire}}{i_g i_f} \\
&T_{Mot\_min} < T_{Mot} < T_{Mot\_max} \\
&n_{Mot} = \frac{u i_g i_f}{2\pi R_{tire}} \\
&n_{Mot\_min} < n_{Mot} < n_{Mot\_max} \\
&P_{bat} = \frac{T_{Mot} n_{Mot}}{\eta_{Mot}} \\
&i_g \in \{i_{g1}, i_{g2}, i_{g3}, i_{g4}\} \\
&a_{min} < a < a_{max} \\
&0 < u < u_{max}
\end{aligned} \tag{14}
$$

where m is the mass of the vehicle, R_{tire} is the radius of the tire, and i_f is the final gear ratio, and a represents the acceleration. In this mining condition, the minimum and maximum acceleration are –0.7 m/s^2 and 0.7 m/s^2, and the maximum velocity is 30 km/h.

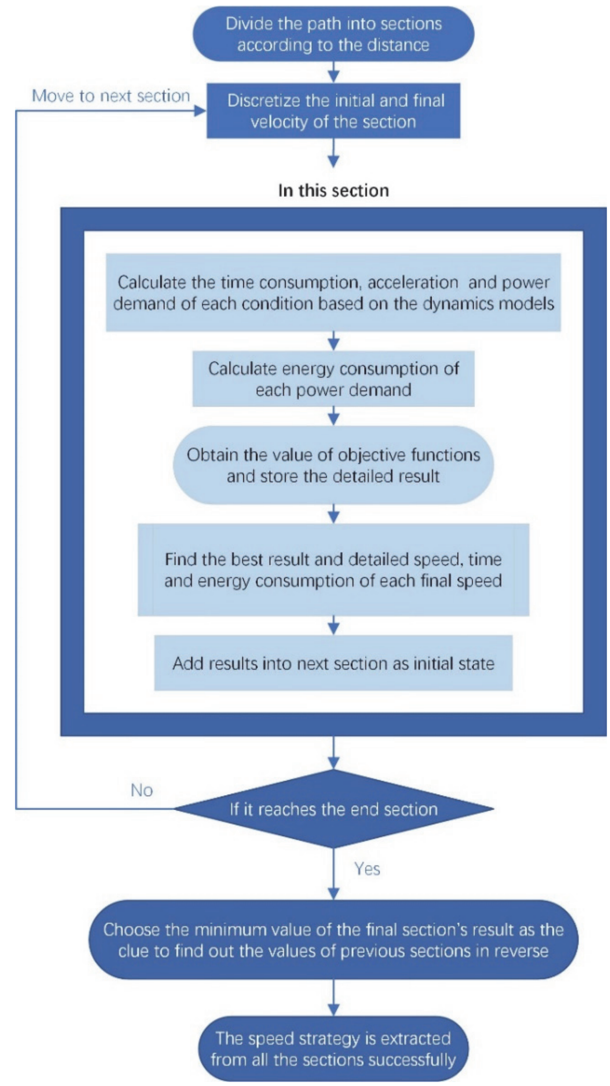

Figure 11. Flowchart for DP optimization.

DP is used to solve this problem. The minimum velocity change V_p is set as 5 km/h. As shown in Figure 11, each final velocity's best result and detailed speed, time, and energy consumption will be stored and added into the next section as the initial state. After all the sections have been calculated, the minimum value of the last section's result is chosen as the clue to find out the values of previous sections in reverse. Then the velocity trajectory is extracted from all the sections successfully.

Figures 12 and 13 show fuel vehicle's velocity trajectory under fuel consumption objective. The time and fuel consumptions are 924.6 s and 3660.1 g for Route 1, respectively, 1236.7 s and 7587.4 g for Route 2. Both velocity trajectories first accelerate to reach the maximum velocity in a period, then adopt the PnG approach frequently to make the engine work in high-efficiency conditions.

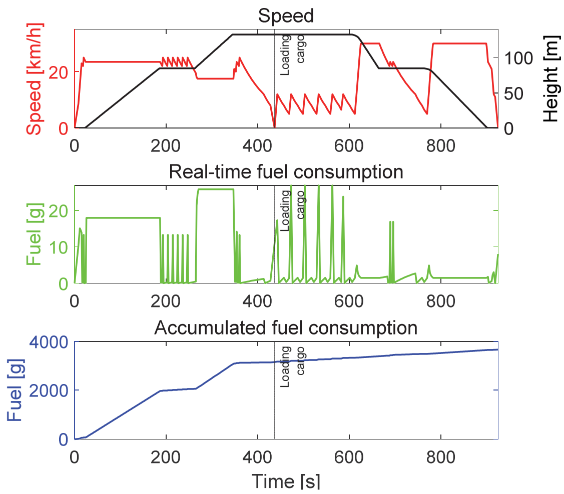

Figure 12. Velocity trajectory of fuel vehicles optimized by the fuel consumption objective for Route 1.

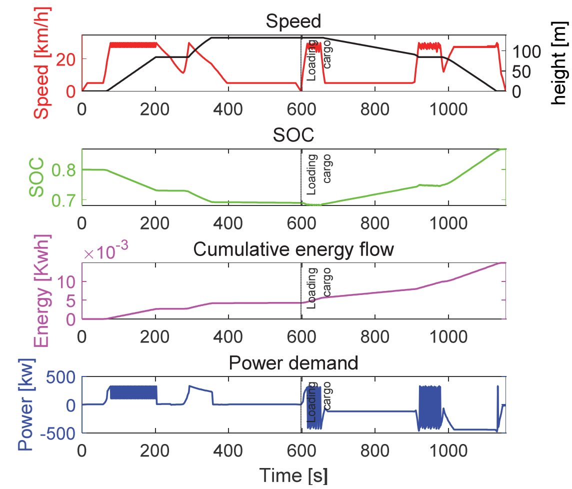

Figure 14. Velocity trajectory of electric vehicles optimized by the fuel consumption objective for Route 1.

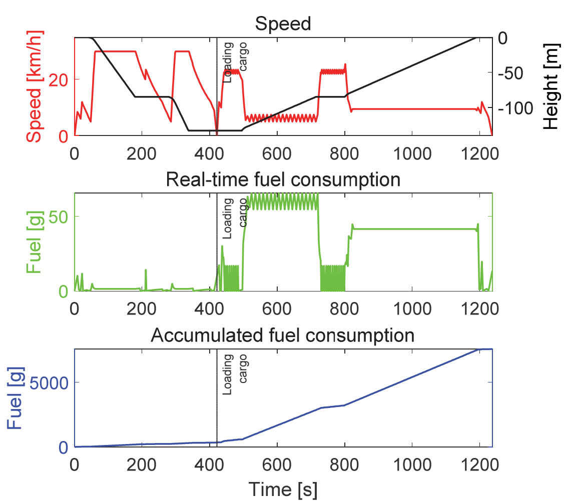

Figure 13. Velocity trajectory of fuel vehicles optimized by the fuel consumption objective for Route 2.

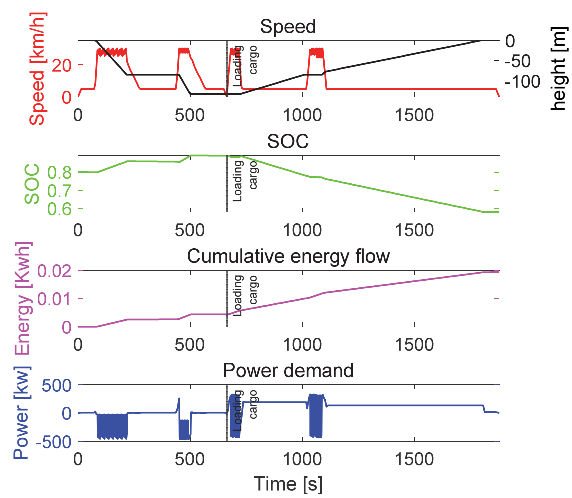

Figure 15. Velocity trajectory of electric vehicles optimized by the fuel consumption objective for Route 2.

The electric vehicle's velocity trajectory optimized by the electricity consumption objective also adopt the PnG approach for both routes, which makes the motor work near the high-efficiency range as long as possible, as shown in Figures 14 and 15. The reduction of electricity is achieved mainly by frequent energy recovery when gliding. It is similar to the trajectories of fuel vehicles optimized by energy consumption objective. Battery SOC increased by 0.0679 for Route 1 but decreased by 0.2205 for Route 2. It takes 1156.4 s to complete Route 1 and 1879.0 s for Route 2. For Route 1, the energy recovered from going downhill with a full load is enough to compensate for the energy consumption when going uphill, so battery SOC increases eventually.

4.2. Multi-objective Optimization

Vehicles have different transportation costs, considered differently in other working conditions. It mainly includes transportation time, energy consumption, wear, and equipment depreciation. The battery's power consumption will lead to a decrease in battery lifetime. Therefore, the energy consumption target of electric vehicles must balance the power battery life loss and power consumption. It is a Pareto-optimal problem. Based on the results of single-objective optimization, the objective of the proposed problem is to minimize energy dissipation, travel time, and battery capacity loss simultaneously under the constraints of terminal braking distance, terminal velocity, and the physical constraints of powertrain components. The multi-

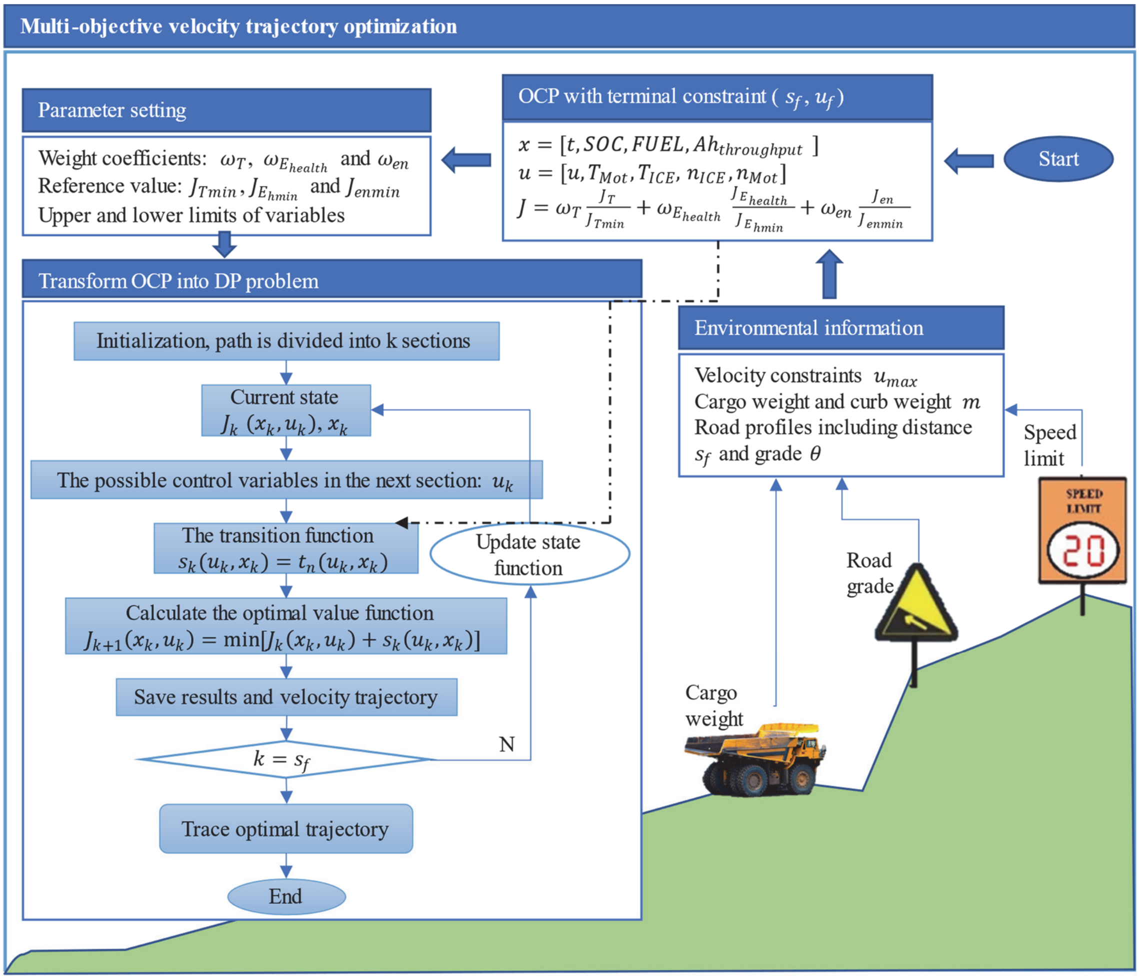

Figure 16. Framework of the multi-objective optimization.

objective optimal mathematical model is constructed with "time consumption," "energy consumption," and "battery lifetime" as the optimization objectives in the following. The framework of the multi-objective optimization is shown in Figure 16.

The formula of multiple objectives proposed in this paper is linear, and the normalized multi-objective function considering travel time, energy consumption, and battery health is shown as follows:

$$J = \omega_T \frac{J_T}{J_{Tmin}} + \omega_{E_{health}} \frac{J_{E_{health}}}{J_{E_{hmin}}} + \omega_{en} \frac{J_{en}}{J_{enmin}} \tag{15}$$

where J_T, $J_{Ehealth}$, and J_{en} are travel time, battery loss and energy consumption of the objective function, ω_T, $\omega_{Ehealth}$, and ω_{en} represent their weights. $\omega_{Ehealth}$ can be set as 0 if it is a fuel vehicle. J_{Tmin}, J_{Ehmin}, and J_{enmin} are the reference value which is the minimum cost optimized by their single objective as discussed in Section 4.1. The function of J_{en} depends on the type of vehicle, as shown in Equations (13) and (14). For the fuel vehicle, J_{en} represent the fuel consumption. However, it is the change of SOC for the electric vehicle.

From the Equation (15), J_T represents the objective function of travel time, as shown in Equation (16). When the vehicle driving trajectory consumes the least time, that is, $J_T = J_{Tmin}$. The objective function of travel time is equal to 1 at this point. While in other cases, the time consumption J_T is more than J_{Tmin}. The objective function of travel time is greater than 1. Therefore, the smaller the value of J_T / J_{Tmin} is, and the closer it is to 1, the shorter travel time will be and the more efficient the speed trajectory will be. Similarly, vehicles' energy consumption and battery loss can be normalized to obtain the formula. The closer the value of J_T, $J_{Ehealth}$, and J_{en} are to the reference value, the lower the objective function of the velocity trajectory is.

$$J_T = \int_{s_0}^{s_f} \frac{ds}{u} \tag{16}$$

Studies have shown that the decay of battery loss is related to the cumulative ampere-hour flow (Cordoba-Arenas *et al.*, 2015; Wang *et al.*, 2011). The cumulative ampere-hour flow can measure the degree of battery aging. The expression for cumulative ampere-hour flow $Ah_{throughput}$ throughput of battery is as follows.

$$Ah_{throughput} = n_b \int_{s_0}^{s_f} |i_b| \frac{ds}{u} \tag{17}$$

where n_b is the number of series of the battery pack, and i_b is the current of each battery series.

Considering the relatively large calculations of the $Ah_{throughput}$ current, the cumulative energy flow $E_{throughput}$ of the battery pack is used as the basis for measuring battery losses. The relationship between $E_{throughput}$ and $Ah_{throughput}$ is expressed as follows.

$$E_{throughput} = \int_{s_0}^{s_f} |P_{bat}| \frac{ds}{u} = n_b \int_{s_0}^{s_f} |V_{oc} i_b| \frac{ds}{u} = n_b \overline{V_{oc}} \int_{s_0}^{s_f} |i_b| \frac{ds}{u} = \overline{V_{oc}} Ah_{throughput} \tag{18}$$

The objective function of battery lifetime is shown in Equation (19). Thus, the single-objective optimal control problems of fuel and electric vehicles within the existing constraints are formulated as Equations (20) and (21).

$$J_{E_{health}} = \int_{s_0}^{s_f} |P_{bat}| \frac{ds}{u} \tag{19}$$

$$J_{Fuel} = \omega_T \frac{\int_{s_0}^{s_f} \frac{ds}{u}}{J_{Tmin}} + \omega_{en} \frac{\int_{s_0}^{s_f} Fuel \cdot P_{out} \frac{ds}{u}}{J_{enmin}}$$

$$s.t.$$

$$\begin{aligned}
&\frac{du}{ds} = \frac{F_{trac} - F_i - F_j - F_{aero} - F_{roll}}{mu} \\
&a = \frac{udu}{ds} \\
&T_{ICE} = \frac{F_{trac} R_{tire}}{i_g i_f} \\
&T_{ICE_min} < T_{ICE} < T_{ICE_max} \\
&n_{ICE} = \frac{u i_g i_f}{2\pi R_{tire}} \\
&n_{ICE_min} < n_{ICE} < n_{ICE_max} \\
&i_g \in \{i_{g1}, i_{g2}, i_{g3}, i_{g4}, i_{g5}, i_{g6}\} \\
&a_{min} < a < a_{max} \\
&0 < u < u_{max}
\end{aligned} \tag{20}$$

$$J_{Elec} = \omega_T \frac{\int_{s_0}^{s_f} \frac{ds}{u}}{J_{Tmin}} + \omega_{E_{health}} \frac{\int_{s_0}^{s_f} |P_{bat}| \frac{ds}{u}}{J_{E_{hmin}}} + \omega_{en} \frac{\int_{s_0}^{s_f} \frac{U_{OC} - \sqrt{U_{OC}^2 - 4P_{bat}R_{eq}}}{2R_{eq}Q_{max}} \frac{ds}{u}}{J_{enmin}}$$

$$s.t.$$

$$\begin{aligned}
&\frac{du}{ds} = \frac{F_{trac} - F_i - F_j - F_{aero} - F_{roll}}{mu} \\
&a = \frac{udu}{ds} \\
&T_{Mot} = \frac{F_{trac} R_{tire}}{i_g i_f} \\
&T_{Mot_min} < T_{Mot} < T_{Mot_max} \\
&n_{Mot} = \frac{u i_g i_f}{2\pi R_{tire}} \\
&n_{Mot_min} < n_{Mot} < n_{Mot_max} \\
&P_{bat} = \frac{T_{Mot} n_{Mot}}{\eta_{Mot}} \\
&i_g \in \{i_{g1}, i_{g2}, i_{g3}, i_{g4}\} \\
&a_{min} < a < a_{max} \\
&0 < u < u_{max}
\end{aligned} \tag{21}$$

In this mining scenario, the a_{min} and a_{max} are –0.7 m/s^2 and 0.7 m/s^2, and the u_{max} is 30 km/h. The reference value J_{Tmin}, J_{Ehmin}, and J_{enmin} of fuel and electric vehicles are obtained by the single-optimization results under their objectives, as discussed in Section 4.1. The detailed optimization results of Route 1 and Route 2 are shown in Tables 4 and 5, where the number underlined can be set as the reference value. The analysis of the results will be discussed in the next section. Therefore, J_{Tmin} and J_{enmin} are set as 628.6 and 3660.1 for Route 1 as the fuel vehicle, respectively. Meanwhile, 825.6 and 7587.4 for Route 2. It is similar to electric vehicles. J_{Tmin}, J_{Ehmin}, and J_{enmin} are 635.5, 28.7, and 0.0679 for Route 1, respectively. Reference values are 1403.3, 55.0, and 0.2205 for Route 2.

Simulations are carried out to verify the effectiveness of the proposed multi-objective optimization method using the DP algorithm. ω_T, $\omega_{Ehealth}$, and ω_{en} are set as 1, except that $\omega_{Ehealth}$ is 0 for fuel vehicles. The results of fuel vehicles

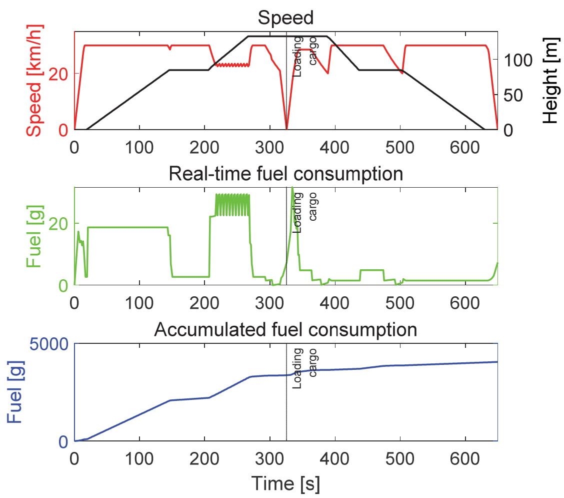

Figure 17. Velocity trajectory of fuel vehicles optimized by multi-objective for Route 1.

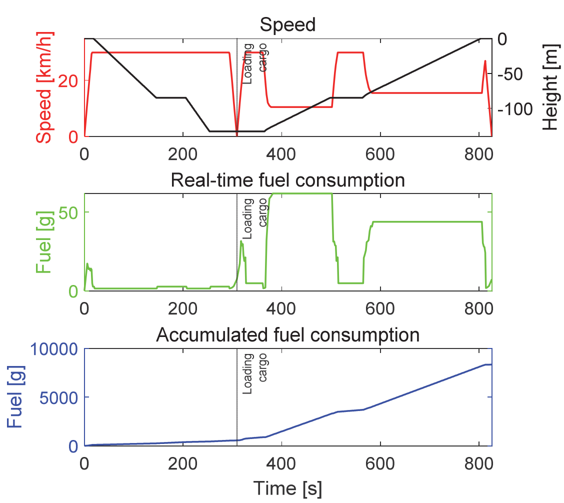

Figure 18. Velocity trajectory of fuel vehicles optimized by multi-objective for Route 2.

optimized by multi-objective DP are shown in Figures 17 and 18. As depicted in Figures, the velocity trajectory also showed a slight PnG phenomenon, especially in going uphill scenarios, to balance time and fuel consumption optimization objectives. Multi-objective optimization for electric vehicles includes travel time, electricity consumption, and battery loss. As shown in Figures 19 and 20, the PnG trajectory is still being used in the optimized velocity trajectory during going uphill and downhill, obviously. It offers a specific correlation between speed trajectory and gradient; it will adopt different frequencies of the PnG approach as the gradient changes. The detailed results about energy consumption, travel time, and battery loss are displayed in Tables 4 and 5.

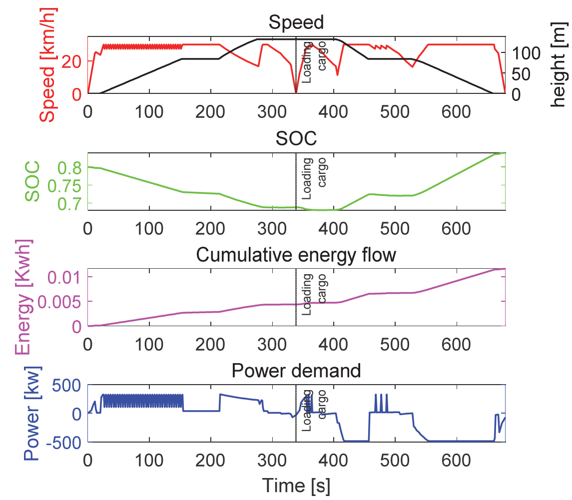

Figure 19. Velocity trajectory of electric vehicles optimized by multi-objective for Route 1.

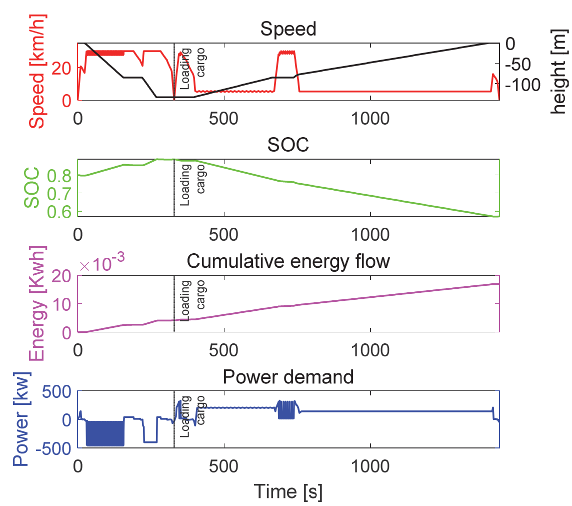

Figure 20. Velocity trajectory of electric vehicles optimized by multi-objective for Route 2.

5. COMPARISON AND DISCUSSION

To applicate the multi-objective formula, some reference values, J_{Tmin}, J_{Ehmin}, and J_{enmin}, need to be obtained by the single-objective optimization. Thus, simulations about travel time and battery loss objective are carried out for both vehicle models using the single-objective approach discussed in Section 4.1 individually, such as "time consumption" and "battery lifetime." A mining road scenario is considered in this paper, whose constraints are the same as the condition described in Section 2. The velocity trajectories of vehicles optimized by "time consumption" and "battery lifetime" are depicted in Figures 21 ~ 26.

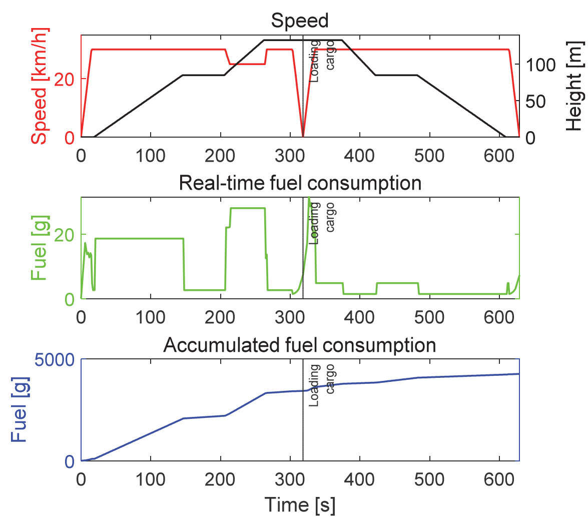

Figure 21. Velocity trajectory of fuel vehicles optimized by time consumption for Route 1.

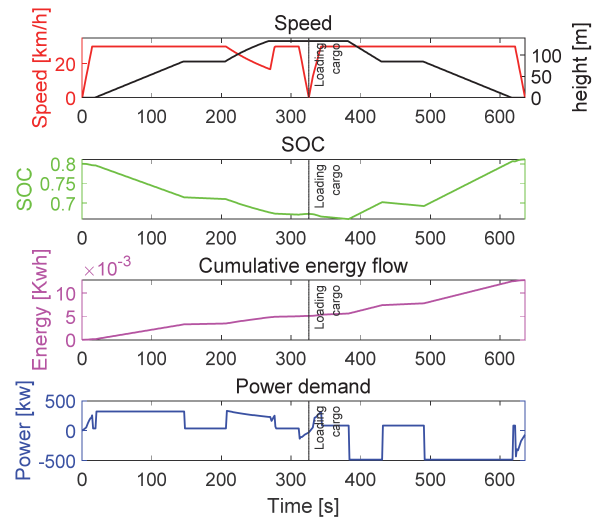

Figure 23. Velocity trajectory of electric vehicles optimized by time consumption for Route 1.

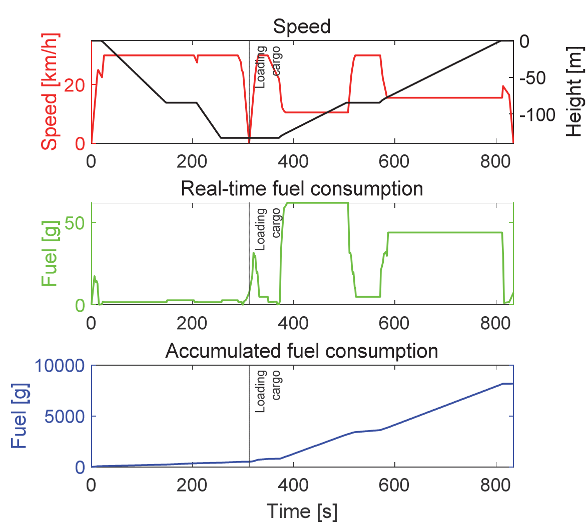

Figure 22. Velocity trajectory of fuel vehicles optimized by time consumption for Route 2.

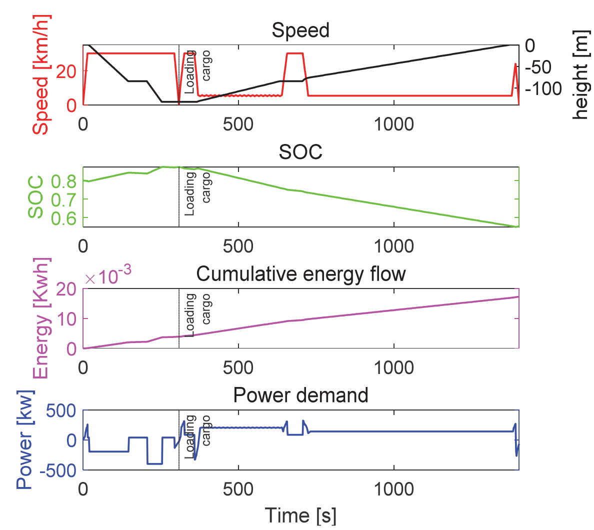

Figure 24. Velocity trajectory of electric vehicles optimized by time consumption for Route 2.

The optimization objectives of Figures 21 ~ 24 are about time consumption. It can be found that the velocity trajectories of both vehicles tend to reach maximum speed, passing the entire route as fast as possible with minor fluctuations to minimize travel time when time consumption is set as the single optimization objective. The engine or motor always operates at the maximum torque the external characteristic curve allows. However, it decelerates the velocity to protect the engine and motor in case of the demand power exceeds the power limit when going uphill. Figures 25 and 26 show that the optimized cumulative energy flow decreased significantly compared with other results, which can extend the battery's lifetime. The optimization results of battery lifetime also adopt the PnG behavior. However, it is different from other optimization results. This PnG trajectory aims to keep the battery in a non-working state as much as possible, neither charged nor discharged.

On the basis of simulation results, the detailed optimization results for both vehicles with different objectives are compiled in Tables 4 and 5. Moreover, the time and energy consumption change are plotted together in Figures 27 ~ 30. The results underlined are the minimum values under single-objective conditions which can be set as the reference value for the multi-objective optimization formula in Section 4.

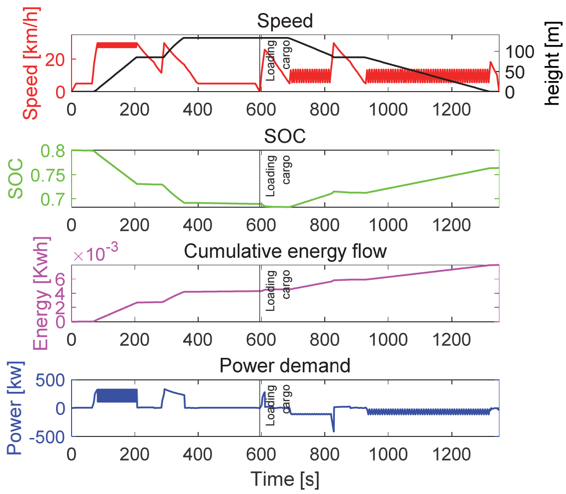

Figure 25. Velocity trajectory of electric vehicles optimized by battery lifetime for Route 1.

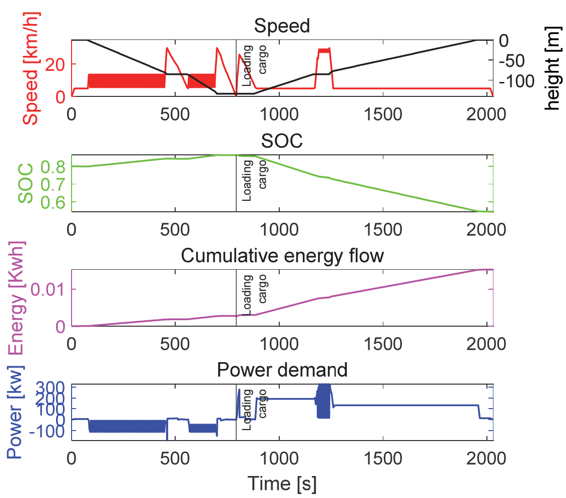

Figure 26. Velocity trajectory of electric vehicles optimized by battery lifetime for Route 2.

Several insights can be drawn from the results of multi-objective optimization for fuel and electric vehicles. Compared with energy priory velocity trajectories, the velocity trajectories optimized by multi-objective spend less time, and it goes more smoothly with fewer velocity fluctuations. Moreover, it can decrease the battery capacity loss prolonging the battery's lifetime for electric vehicles. However, it leads to an increment in energy consumption. For fuel vehicles, it can decrease the time consumption by 29.74 % on Route 1 and 32.54 % on Route 2. For electric vehicles, the multi-objective optimized trajectories can decrease the battery capacity loss by 22.01 % and time consumption by 41.28 % on Route 1. It also reduces in battery capacity loss and time consumption to an extent on Route 2.

Table 4. Optimized results for Route 1.

Fuel vehicle results			
Optimization objective		Fuel consumption (g)	Travel time (s)
Time objective		4267.0	628.6
Fuel objective		3660.1	924.6
Multi-objective		4041.5	649.6
Electric vehicle results			
Optimization objective	Change of SOC	Cumulative energy flow (Kwh)	Travel time (s)
Time objective	0.0113	46.1	635.5
Electricity objective	0.0679	53.6	1156.4
Battery lifetime objective	-0.0361	28.7	1349.9
Multi-objective	0.0393	41.8	679.0

Table 5. Optimized results for Route 2.

Fuel vehicle results			
Optimization objective		Fuel consumption (g)	Travel time (s)
Time objective		8347.4	825.6
Fuel objective		7587.4	1236.7
Multi-objective		8170.4	834.3
Electric vehicle results			
Optimization objective	Change of SOC	Cumulative energy flow (Kwh)	Travel time (s)
Time objective	-0.2478	61.9	1403.3
Electricity objective	-0.2205	69.4	1879.0
Battery lifetime objective	-0.2545	55.0	2030.8
Multi-objective	-0.2298	60.6	1440.9

As depicted in Figures 27 ~ 30, when transport time is set as single objective, there is an apparent linear relationship between the travel time and distance of the two vehicles. The gradient of the curve is slight and does not fluctuate significantly, which means vehicles pass the route at a constant speed as fast as possible, but it leads to high energy consumption. When energy consumption or battery lifetime is set as the single objective, the optimal driving speed trajectory shows a particular association with the slope. The curve of time consumption and distance has nonlinear

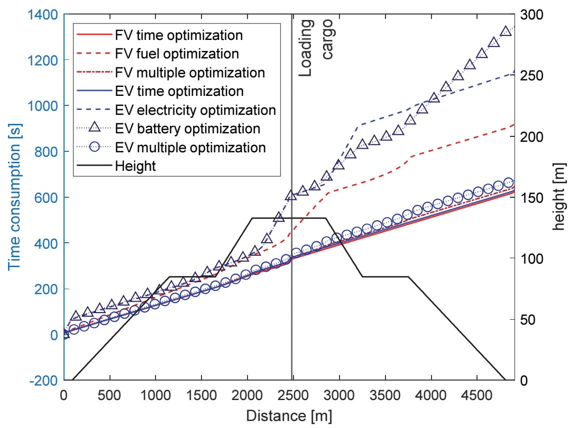

Figure 27. Time consumption of different driving strategies for Route 1.

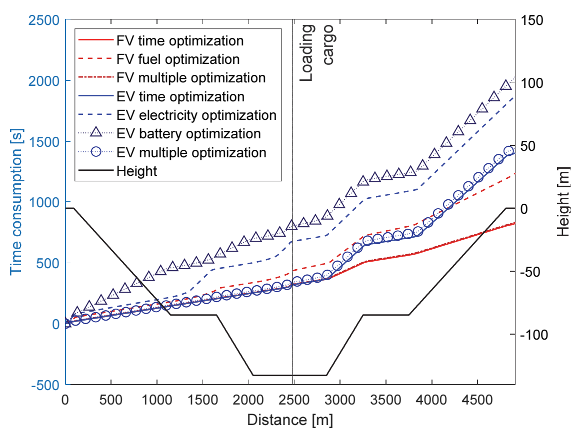

Figure 28. Time consumption of different driving strategies for Route 2.

characteristics. It presents different gradients under different slopes. The energy consumption is at a relatively low state. When conducting multi-objective optimization, both vehicles adopt PnG trajectories. It is different from any single-objective optimization result. The time consumption curve is nonlinear and finds a trade-off between the time optimization and energy optimization.

Energy and time consumptions have contradictory characteristics to a certain extent and are directly correlated to vehicle velocity. Reducing energy consumption requires sacrificing driving time and vice versa. It is similar to battery loss. The reduction of electricity is achieved by frequent energy recovery. It causes an increase in cumulative energy flow and loss of battery lifetime. Nevertheless, battery lifetime is optimized by reducing the frequency of charging and discharging. There is a compromise between the loss of battery lifetime and electricity consumption.

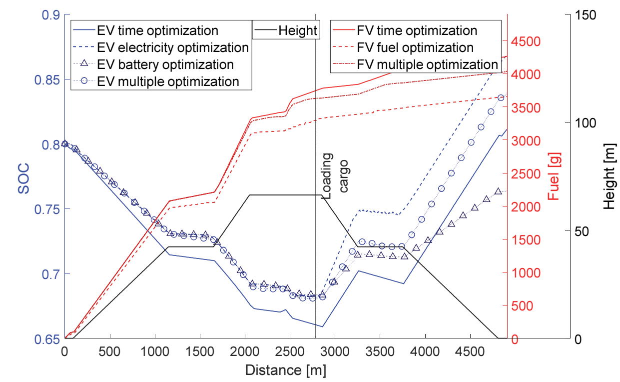

Figure 29. Energy consumption of different driving strategies for Route 1.

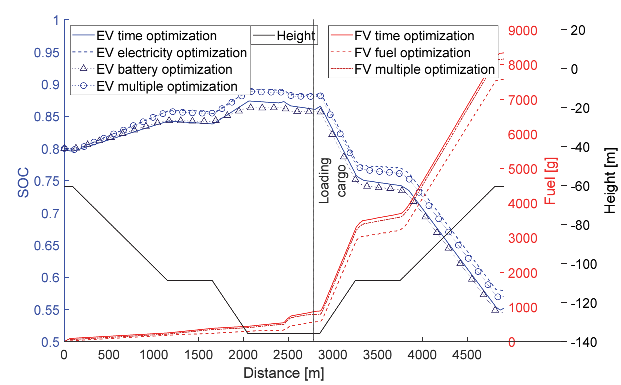

Figure 30. Energy consumption of different driving strategies for Route 2.

The objectives of mining vehicle transportation are so complex that it is difficult to find a fixed formula to calculate. It achieved different Pareto optimal trade-offs between them. The multi-objective solutions are analyzed to exhibit the trade-off between “time consumption,” “energy consumption,” and “battery lifetime,” which assists in finding a desired solution.

6. CONCLUSION

The driving speed trajectory of mining vehicles under driverless conditions has more optimization space. It is yet to be involved in the previous energy-saving research for mining vehicles. In this paper, we discuss velocity trajectory optimization for autonomous mining vehicles. The following conclusions can be made from the above research.

(1) A multi-objective optimization method using DP was proposed considering travel time, energy consumption, and battery lifetime. Its effectiveness and appropriateness are verified on the fuel and electric vehicle models.

Thus, it is more suitable for the cost management of mine transportation in the actual closed open-pit mine condition.

(2) The multi-objective optimization was carried out in the two mining scenarios using DP, including going uphill and downhill conditions. It's found that a specific correlation between velocity trajectory and the gradient of the route. It will adopt different frequencies of the PnG approach as the gradient of routes changed.

(3) Compared with energy priory velocity trajectories, the results optimized by multi-objective spend less time, and it runs more smoothly with fewer velocity fluctuations. Moreover, it can reduce the battery capacity loss, which prolongs the battery's lifetime for electric vehicles. However, it leads to an increment in energy consumption. It is a kind of Pareto optimal trade-off.

In future work, the composition of objectives and their weights should be investigated more based on accurate mine empirical data utilizing big data and machine learning. The structure of multi-objective optimization can be applied to different transportation scenarios adaptively.

ACKNOWLEDGEMENT–This research was supported by the Scientific and Technological Innovation Foundation of Foshan, USTB. Our deepest gratitude goes to the editors and the anonymous reviewers for their careful work and thoughtful suggestions that contributed considerably to the improvement of this paper.

REFERENCES

Cai, Y., Ouyang, M. and Yang, F. (2017). Energy management and design optimization for a series-parallel PHEV city bus. *Int. J. Automotive Technology* **18**, **3**, 473–487.

Cordoba-Arenas, A., Onori, S., Guezennec, Y. and Rizzoni, G. (2015). Capacity and power fade cycle-life model for plug-in hybrid electric vehicle lithium-ion battery cells containing blended spinel and layered-oxide positive electrodes. *J. Power Sources*, **278**, 473–483.

De Cauwer, C., Verbeke, W., Van Mierlo, J. and Coosemans, T. (2019). A model for range estimation and energy-efficient routing of electric vehicles in real-world conditions. *IEEE Trans. Intelligent Transportation Systems* **21**, **7**, 2787–2800.

Dehkordi, S. G., Larue, G. S., Cholette, M. E., Rakotonirainy, A. and Glaser, S. (2022). Including network level safety measures in eco-routing. *J. Intelligent Transportation Systems*, 1–14.

Gilbert, E. G. (1976). Vehicle cruise: Improved fuel economy by periodic control. *Automatica* **12**, **2**, 159-166.

Guo, L., Chen, H., Liu, Q. and Gao, B. (2019). A computationally efficient and hierarchical control strategy for velocity optimization of on-road vehicles. *IEEE Trans. Systems Man Cybernetics-Systems* **49**, **1**, 31–41.

Hu, J., Li, Z., Zhu, P. and Xiao, F. (2022). Speed trajectory optimization method for electric vehicles based on driving style. *IEEE Trans. Transportation Electrification* **9**, **1**, 1541–1553.

Kusuma, C. F., Budiman, B. A., Nurprasetio, I. P., Islameka, M., Masyhur, A. H., Aziz, M. and Reksowardojo, I. K. (2021). Energy management system of electric bus equipped with regenerative braking and range extender. *Int. J. Automotive Technology* **22**, **6**, 1651–1664.

Liu, R., Liu, H., Han, L., He, P. and Zhang, Y. (2023). A multi-objective regenerative braking control strategy combining with velocity optimization for connected vehicles. *Proc. Institution of Mechanical Engineers, Part D: J. Automobile Engineering* **237**, **6**, 1465–1474.

Ma, J., Hu, J., Leslie, E., Zhou, F., Huang, P. and Bared, J. (2019). An eco-drive experiment on rolling terrains for fuel consumption optimization with connected automated vehicles. *Transportation Research Part C: Emerging Technologies*, **100**, 125–141.

Patterson, S. R., Kozan, E. and Hyland, P. (2017). Energy efficient scheduling of open-pit coal mine trucks. *European J. Operational Research* **262**, **2**, 759–770.

Wang, J., Liu, P., Hicks-Garner, J., Sherman, E., Soukiazian, S., Verbrugge, M., Tataria, H., Musser, J. and Finamore, P. (2011). Cycle-life model for graphite-$LiFePO_4$ cells. *J. Power Sources* **196**, **8**, 3942–3948.

Wu, J., He, H., Peng, J., Li, Y. and Li, Z. (2018). Continuous reinforcement learning of energy management with deep Q network for a power split hybrid electric bus. *Applied Energy*, **222**, 799–811.

Xu, B., Chen, X., Li, K., Hu, M., Bian, Y., Yu, Q. and Wang, J. (2019). Double-layer speed optimization for reducing fuel consumption with vehicle-to-infrastructure communication. *J. Intelligent Transportation Systems* **23**, **5**, 513–524.

Xu, S., Li, S. E., Zhang, X., Cheng, B. and Peng, H. (2015). Fuel-optimal cruising strategy for road vehicles with step-gear mechanical transmission. *IEEE Trans. Intelligent Transportation Systems* **16**, **6**, 3496–3507.

Zhang, S. and Xiong, R. (2015). Adaptive energy management of a plug-in hybrid electric vehicle based on driving pattern recognition and dynamic programming. *Applied Energy*, **155**, 68–78.

Zhu, G., Lin, J., Liu, Q. and He, H. (2019). Research on the energy-saving strategy of path planning for electric vehicles considering traffic information. *Energies* **12**, **19**, 3601.